THE CAMBRIDGE ENCYCLOPEDIA OF THE SUN

Kenneth R. Lang
Tufts University, Medford, Massachusetts, USA

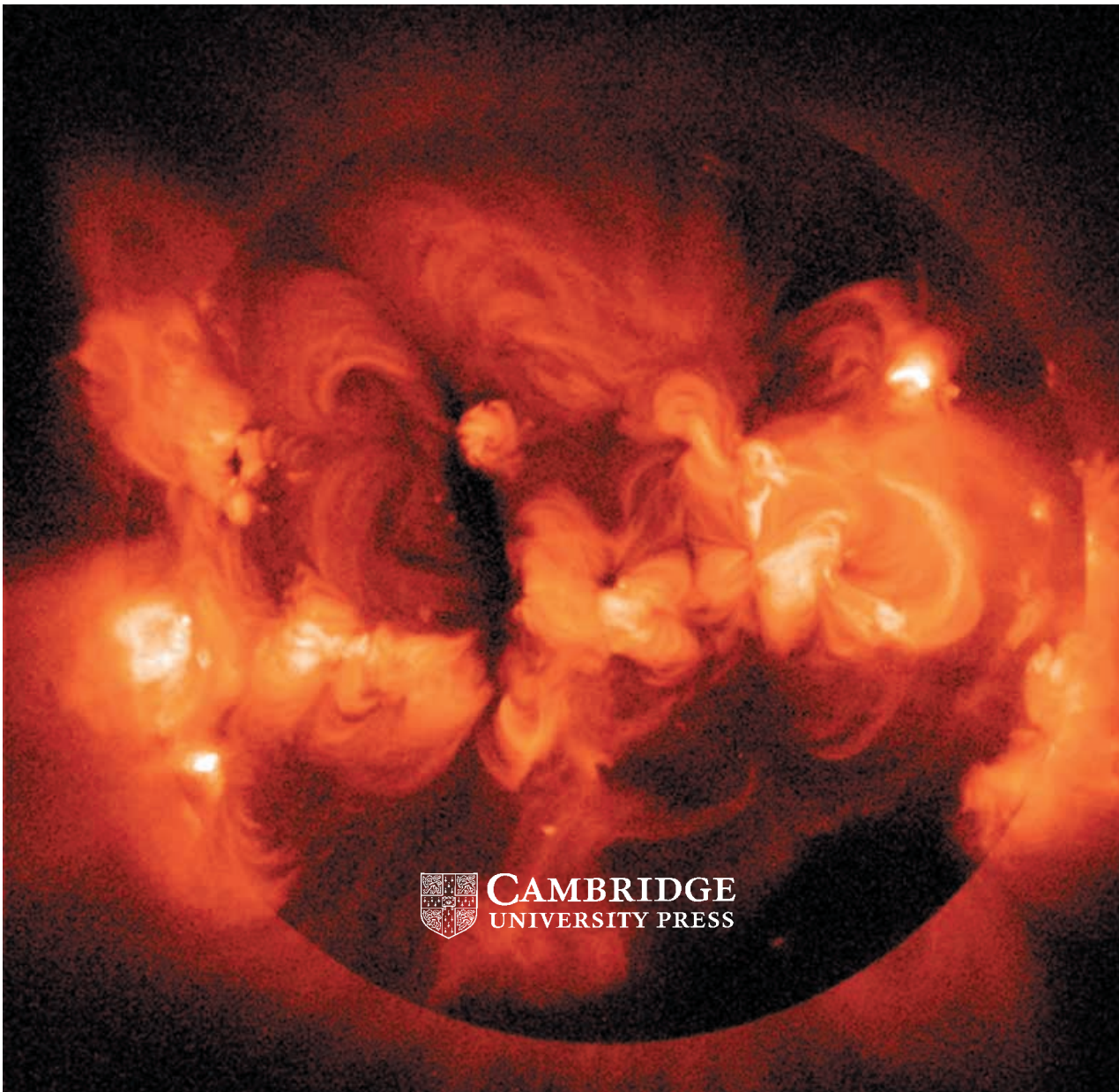

PUBLISHED BY THE PRESS SYNDICATE OF THE UNIVERSITY OF CAMBRIDGE
The Pitt Building, Trumpington Street, Cambridge, United Kingdom

CAMBRIDGE UNIVERSITY PRESS
The Edinburgh Building, Cambridge CB2 2RU, UK
40 West 20th Street, New York, NY 10011-4211
10 Stamford Road, Oakleigh, VIC 3166, Australia
Ruiz de Alarcón 13, 28014 Madrid, Spain
Dock House, The Waterfront, Cape Town 8001, South Africa

http://www.cambridge.org

First published 2001

Printed in the United Kingdom at the University Press, Cambridge

Typeface Joanna 10.25/12.5pt. *System* QuarkXpress

A catalogue record for this book is available from the British Library

Library of Congress cataloguing in Publication data

Lang, Kenneth R.
The Cambridge Encyclopedia of the Sun/Kenneth R. Lang
p. cm.
Includes bibliographical references and index.
ISBN 0 521 78093 4
1. Sun–Encyclopedias. 1. Title.
QB521.L24 2001
523.7′03–dc21 00-049365

ISBN 0 521 78093 4 hardback

Contents

Chapter Six

The explosive Sun

A filament erupts A filament is shown in the process of lifting off from the edge of the Sun – north is to the left. The dark matter is relatively cool, around 20 000 degrees kelvin, while the bright material is at a temperature of a million degrees kelvin or more. From top to bottom, the structure stands 120 million (1.20×10^8) meters tall. This image was taken from the *Transition Region And Coronal Explorer*, *TRACE*, on 19 July 2000 at a wavelength of 17.1 nm. (Courtesy of the *TRACE* consortium, the Stanford-Lockheed Institute of Space Research, and NASA.)

6.1 Solar flares

Active regions are the sites of sudden and brief explosions, called solar flares, that rip through the atmosphere above sunspots with unimagined intensity. In just 100 to 1000 seconds, the disturbance can release an energy of 10^{24} joule. A single flare then creates an explosion equivalent to 2.5 million terrestrial nuclear bombs, each with a destructive force of 100 megatons (10^{11}kg) of trinitrotoluene, or TNT. All of this power is created in a relatively compact explosion, comparable in total area to a sunspot, and occupying less than one-ten-thousandth (0.01 percent) of the Sun's visible disk.

For a short while, a flare can be the hottest place on the Sun, heating Earth-sized active regions to tens of millions of degrees kelvin. The explosion floods the solar system with intense radiation across the full electromagnetic spectrum, from the shortest X-rays to the longest radio waves.

Although flares appear rather inconspicuous in visible light, they can briefly produce more X-ray and radio radiation than the entire non-flaring Sun does at these wavelengths. We can use this radiation to watch the active-region atmosphere being torn asunder by the powerful explosions; and then view the lesion being stitched together again.

During the sudden and brief outbursts, electrons and protons can be accelerated to nearly the speed of light. Protons and helium nuclei are thrown down into the chromosphere, generating nuclear reactions there. The high-speed electrons and protons are also hurled out into interplanetary space where they can threaten astronauts and satellites. Shock waves can be produced during the sudden, violent release of flare energy, ejecting masses of hot coronal gas into interplanetary space. Some of the intense radiation and energetic particle emissions reach the Earth where they can adversely affect humans (Section 8.3).

Since flares occur in active regions, their frequency follows the 11-year magnetic-activity cycle. The rate of solar flares of a given energy increases by about an order of magnitude, or a factor of ten, from the cycle minimum to its maximum. At the cycle maximum, scores of small flares and several large ones can be observed each day. Yet, even at times of maximum solar activity, the most energetic flares remain infrequent, occurring only a few times a year; like rare vintages, they are denoted by their date. Flares of lesser energy are much more common. Those with half the energy of another group occur about four times as often.

Solar flares are always located near sunspots and occur more often when sunspots are most numerous. This does not mean that sunspots cause solar flares, but it does suggest that solar flares are energized by the powerful magnetism associated with sunspots. When the magnetic fields in a solar active region become contorted, magnetic energy is built up and stored in the low corona. When the pent-up energy is released it is often in the form of a solar flare. This energy is suddenly and explosively released at higher levels in the solar atmosphere just above sunspots.

Flares in the chromosphere

Our perceptions of solar flares have evolved with the development of new methods of looking at them. Despite the powerful cataclysm, most solar flares are not, for example, detected on the bland white-light face of the Sun. They are only minor perturbations in the total amount of emitted sunlight; every second the photosphere emits an energy of 3.85×10^{26} J, far surpassing the total energy emitted by any solar flare by at least a factor of one hundred.

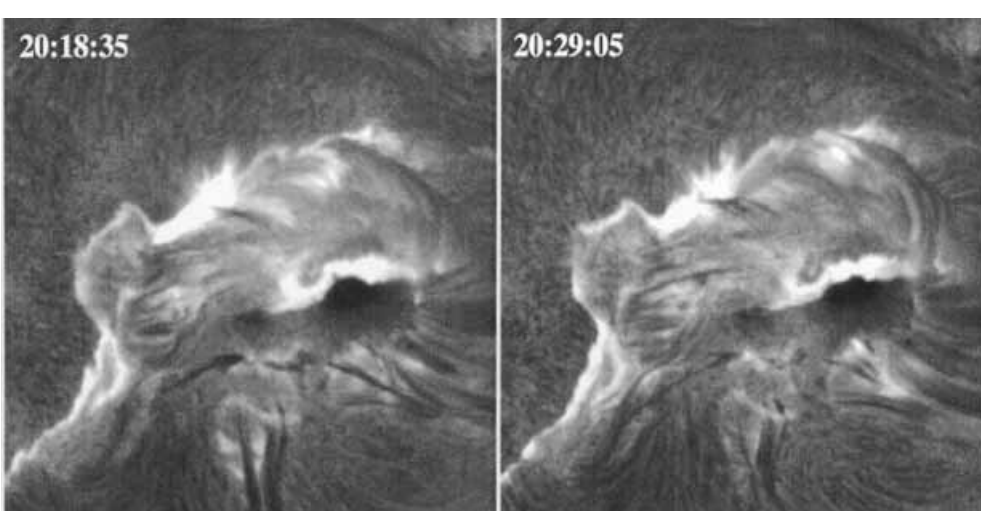

Fig. 6.1 **Hydrogen-alpha flare ribbons** A large solar flare observed in the red light of hydrogen alpha (Hα), showing two extended, parallel flare ribbons in the chromosphere. Each image is 200 million meters in width, subtending an angle of 300 seconds of arc or about one-sixth of the angular extent of the Sun. These photographs were taken at the Big Bear Solar Observatory on 29 April 1998. (Courtesy of Haimin Wang.)

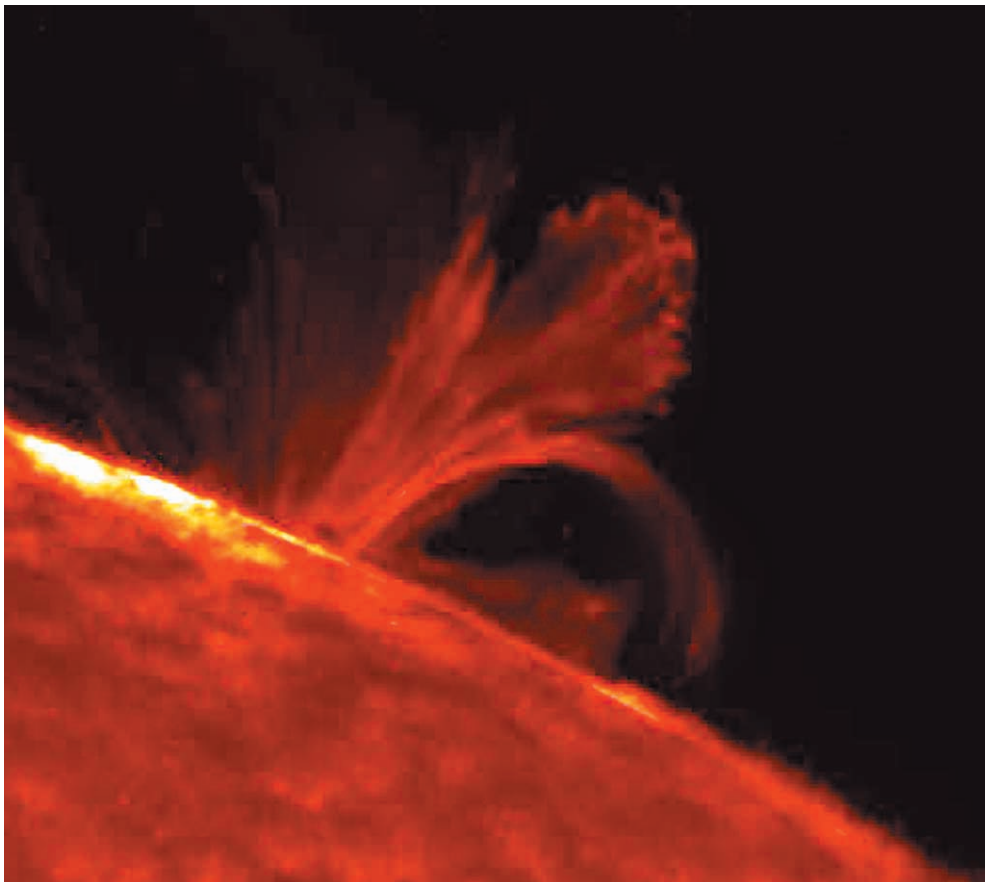

Fig. 6.2 **Lyman-alpha explosion** A flare moves to a height of 150 million meters at the edge of the Sun, shining in the light of the Lyman-alpha emission from hydrogen atoms at 121.6 nm. The emitting gas is at a temperature of 10 000 to 20 000 K, characteristic of the chromosphere. This image shows that flare radiation is emitted from numerous long, thin magnetic filaments. It was taken on 19 May 1998 from *TRACE*, a mission of the Stanford-Lockheed Institute for Space Research and part of the NASA Small Explorer Program. (Courtesy of the *TRACE* consortium and NASA.)

Thus, only exceptionally powerful solar flares can be detected in visible sunlight. These white-light flares, as they are now called, were first observed and carefully recorded by two Englishmen, Richard C. Carrington and Richard Hodgson, who noticed an intense flash of light near a complex group of sunspots on 1 September 1859, lasting just a few minutes.

Routine visual observations of solar explosions were made possible by tuning into the red emission of hydrogen alpha, designated Hα, at a wavelength of 656.3 nm, and rejecting all the other colors of sunlight. Light at this wavelength originates just above the photosphere, in the chromospheric layer of the solar atmosphere. For more than half a century, astronomers throughout the world have used filters to isolate the Hα emission, carrying out a vigilant flare patrol that continues today. Most solar observatories now have automated Hα telescopes, and some of them are used to monitor the Sun for solar flares by capturing images of the Sun every few seconds.

When viewed in this way, solar flares appear as a sudden brightening, lasting from a few minutes to an hour, usually in active regions with strong, complex magnetic fields. The Hα light is not emitted directly above sunspots, but is instead located between regions of opposite magnetic polarity in the underlying photosphere, near the line or place marking magnetic neutrality. Flares in the chromosphere often appear on each side of the magnetic neutral line as two extended parallel ribbons (Fig. 6.1). The two ribbons move apart as the flare progresses, and the space between them is filled with higher and higher shining loops while the lower ones fade away.

The hydrogen-alpha observations describe the shape, size, location and intensity of solar flares in the chromosphere. This leads to one flare classification scheme based on their extent and brightness in Hα (Table 6.1).

The powerful surge of flaring hydrogen light is also detected by spacecraft observing at ultraviolet wavelengths. Detailed magnetic filaments have been resolved in the Lyman-alpha, or Ly α, transition of hydrogen at 121.6 nm (Fig. 6.2).

Yet, a solar flare emits just a modest amount of its power in the chromosphere, and the chromospheric image

Importance	***Flare area*** *(square degrees)*	***Flare area*** *(10^{12} square meters)*	***Flare brilliance***[a]
S (subflare)	Less than 2	Less than 300	f, n, or b
1	2.1 to 5.1	300 to 750	f, n, or b
2	5.2 to 12.4	750 to 1850	f, n, or b
3	12.5 to 24.7	1850 to 3650	f, n, or b
4	More than 24.7	More than 3650	f, n, or b

[a] f = faint; n = normal; b = bright.

Table 6.1 **Hydrogen-alpha classification of solar flares**

Importance	Peak flux at 0.1 to 0.8 nm [a] ($W\ m^{-2}$)
A	10^{-8} to 10^{-7}
B	10^{-7} to 10^{-6}
C	10^{-6} to 10^{-5}
M	10^{-5} to 10^{-4}
X	10^{-4} and above

[a] A number following the letter gives the peak flux in the first unit. For example, X5.2 stands for a peak soft X-ray flux of 5.2×10^{-4}, or 0.000 52, W m^{-2}.

Table 6.2 **Soft X-ray classification of solar flares measured near the Earth**

provides only a two-dimensional, flatland picture without information about what is happening above or below it. Observations at X-ray and radio wavelengths provide new perspectives, leading to a more complete understanding of solar flares. We can tune into flares at these wavelengths and see them in different forms, providing a three-dimensional spatial view.

X-ray flares

Since solar flares are very hot, they emit the bulk of their energy at X-ray wavelengths. For a short while, a large flare can outshine the entire Sun in X-rays (Fig. 6.3). The hot X-ray flare then dominates the background radiation of even the brightest magnetic loops in the quiescent, or non-flaring, solar corona. Because any X-rays coming from the Sun are totally absorbed in the Earth's atmosphere, X-ray flares must be observed from satellites orbiting the Earth above our air.

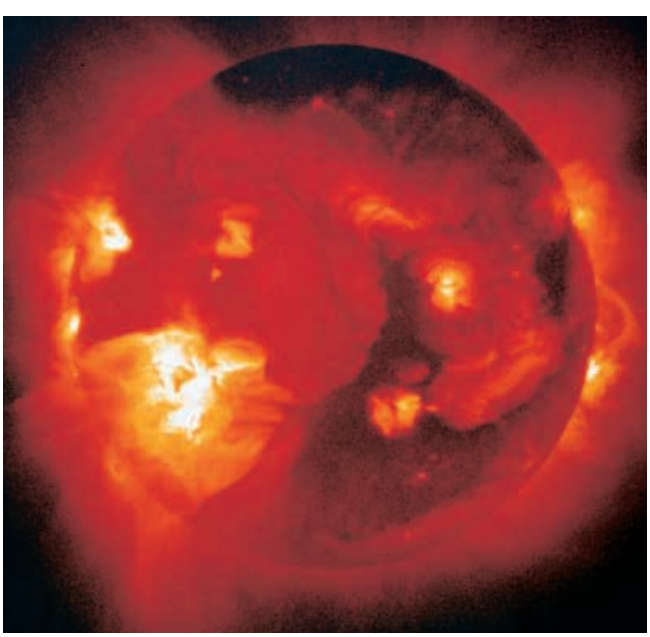

Fig. 6.3 **An X-ray flare** As shown in the lower left of this X-ray image, a solar flare can result in soft X-ray radiation that outshines the entire Sun at these wavelengths. Less luminous coronal loops are found in quiescent, or non-flaring, active regions on other parts of the Sun, and dark coronal holes are also present at both poles (*top* and *bottom*). This image was taken with the Soft X-ray Telescope (SXT) aboard *Yohkoh* on 25 October 1991. (Courtesy of Keith Strong, NASA, ISAS, the Lockheed-Martin Solar and Astrophysics Laboratory, the National Astronomical Observatory of Japan, and the University of Tokyo.)

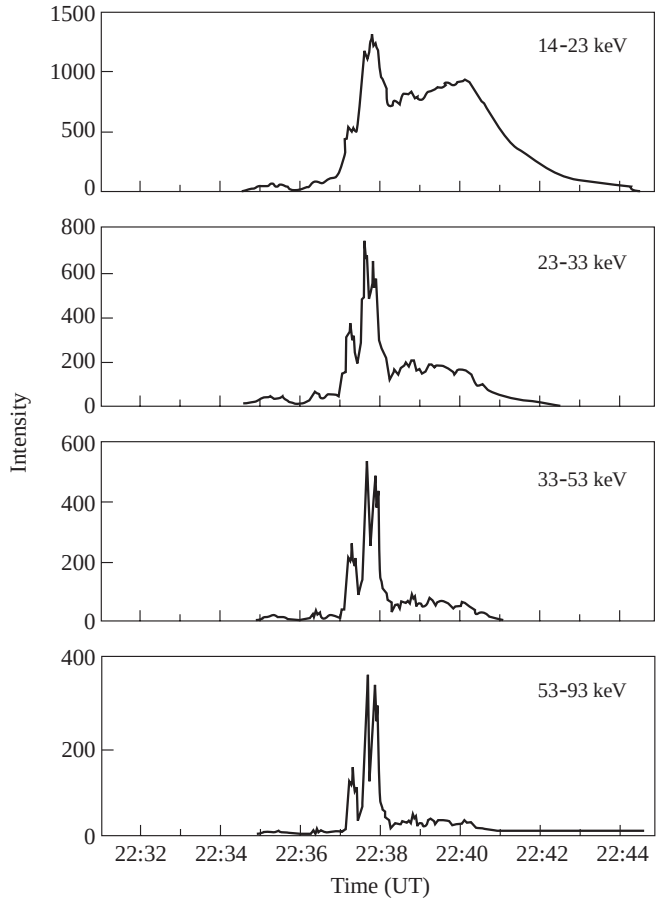

Fig. 6.4 **Impulsive and gradual phases of a flare** The time profile of a solar flare at hard X-ray energies, above 30 keV, is characterized by an impulsive feature that lasts for about one minute. The intensity scale provides the average counting rate, derived from 0.5-second integration, of the 64 imaging elements of the Hard X-ray Telescope (HXT) aboard *Yohkoh*. This impulsive phase coincides with the acceleration of high-speed electrons that emit non-thermal bremsstrahlung at hard X-ray wavelengths and non-thermal synchrotron radiation at centimeter radio wavelengths. The less-energetic emission shown here, below 30 keV, can be composed of two components, an impulsive component followed by a gradual one. The latter component builds up slowly and becomes most intense during the gradual decay phase of solar flares when thermal radiation dominates. At even lower soft X-ray energies (about 10 keV), the gradual phase dominates the flare emission. This data was taken on 15 November 1991. (Courtesy of NASA, ISAS, the Lockheed-Martin Solar and Astrophysics Laboratory, the National Astronomical Observatory of Japan, and the University of Tokyo.)

Hotter gases radiate most intensely at shorter wavelengths, and the wavelength at which the brightness is a maximum, λ_{max}, varies inversely with the temperature, T. The exact relation, known as the Wien displacement law, is given by $\lambda_{max} = 0.002\ 897\ 75/T$ m (Section 1.2, Focus 1.1). A gas heated to ten million degrees kelvin will therefore be brightest at the X-ray wavelength of $\lambda_{max} = 3 \times 10^{-10}$ m = 0.3 nm.

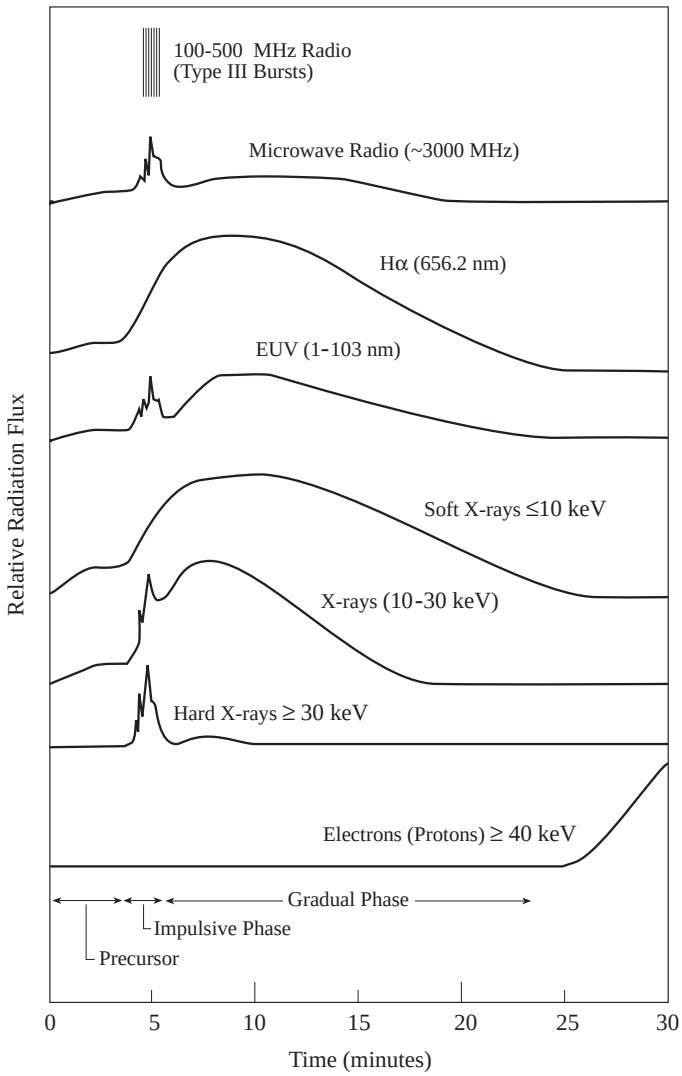

Fig. 6.5 **Solar flares in varying perspectives** During the early impulsive phase of a solar flare, electrons accelerated to high energies and very rapid speeds emit radio bursts, extreme-ultraviolet (EUV) radiation, and hard X-rays. The radio emission is at frequencies from 100 to 3000 MHz, or at wavelengths between 3 and 0.1 m; the hard X-rays have photon energies greater than 30 keV. The subsequent gradual phase is detected with soft X-rays, at energies of about 10 keV or less, as an after-effect of the impulsive radiation. The soft X-rays are the thermal radiation, or bremsstrahlung, of a gas heated to temperatures about ten million degrees kelvin.

Flares can be characterized by their brightness in X-rays, as observed by monitoring satellites near the Earth (Table 6.2). The biggest flares are X-class flares. M-class flares have one tenth the X-ray flux of an X-class one, and the C-class has one hundredth of the X-class flux.

The Space Environment Center of the National Oceanic and Atmospheric Administration, or NOAA, provides the peak soft X-ray flux for solar flares seen from their *Geostationary Operational Environmental Satellites*, or *GOES* for short. These satellites hover above points in the Earth's western hemisphere, orbiting at the same rate that the Earth spins. The flux of electrons and protons striking the satellites is also provided in NOAA's space-weather information, available on the web at **www.sec.noaa.gov**. Space-weather forecasts are discussed further in Section 8.3.

Researchers describe X-rays by the energy they carry. There are soft X-rays with relatively low energy and modest penetrating power. The hard X-rays have higher energy and greater penetrating power. The wavelength of radiation is inversely proportional to its energy, so hard X-rays are shorter than soft X-rays.

The energy of the X-ray radiation is a measure of the energy of the electrons that produce it. In fact, X-rays with a given energy are produced by electrons with roughly the same amount of energy. The energy of both the high-speed electrons and the flaring X-rays is often specified in kilo-electron volts, denoted keV. One keV is equivalent to an energy of 1.6×10^{-16} J, and corresponds to a wavelength of 12.4×10^{-10} m, or 1.24 nm (Focus 1.1). Soft X-rays have energies between 1 and 10 keV, and hard X-rays lie between 10 and 100 keV.

The time profiles of a solar flare depend upon the choice of observing wavelength; when combined they provide detailed information about the physical processes occurring during the lifetime of a solar flare. Hard X-rays are emitted during the impulsive onset of a solar flare, while the soft X-rays gradually build up in strength and peak a few minutes after the impulsive emission (Fig. 6.4). The soft X-rays are therefore a delayed effect of the main flare explosion.

The energetic electrons that produce the impulsive, flaring hard X-ray emission also emit radiation at microwave (centimeter) and radio (meter) wavelengths (Fig. 6.5). The similarity in the time profiles of the microwave and hard X-ray bursts, on time-scales as short as a second, suggests that the electrons that produce both the hard X-rays and the microwaves are accelerated and originate in the same place. Impulsive flare radiation at both the long, hard X-ray wavelengths and the short microwave wavelengths is apparently produced by the same population of high-speed electrons, with energies of 10 to 100 keV.

The *Solar Maximum Mission*, or *SMM* obtained pioneering images in the 1980s of the hard X-rays emitted during the impulsive phase of solar flares. The two-component, or double, hard X-ray sources were concentrated at the footpoints of the coronal loops detected at soft X-ray wavelengths. This is explained if the hard X-rays are generated by energetic, non-thermal electrons hurled down the two legs of a coronal loop into the low corona and dense chromosphere. The discovery of two-centimeter microwave emission at the two footpoints of coronal loops at about the same time supported the hard X-ray double-footpoint evidence.

The slow, smooth rise of the soft X-ray afterglow resembles the time integral of the rapid, impulsive hard X-ray and microwave bursts. This relationship is known as the Neupert effect, named after Werner M. Neupert who first noticed it in 1968 when comparing satellite observations of soft X-ray flares with impulsive microwave bursts observed from the ground.

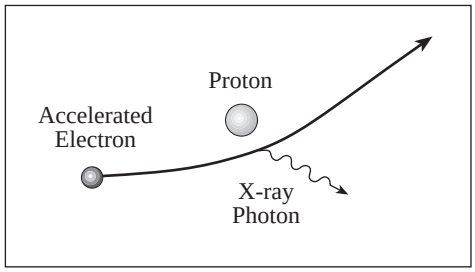

Fig. 6.6 **Bremsstrahlung** When a hot electron moves rapidly and freely outside an atom, it inevitably moves near a proton in the ambient gas. There is an electrical attraction between the electron and proton because they have equal and opposite charge, and this pulls the electron toward the proton, bending the electron's trajectory and altering its speed. The electron emits electromagnetic radiation in the process.

Precise measurements of soft X-ray spectral lines, from the *SMM*, and *P78-1* satellites in the early-1980s, revealed a Doppler shift to shorter wavelengths, suggesting an upward motion of the hot thermal gas at velocities as high as 4×10^5 m s^{-1}. This rise in heated material was explained by a theory called chromospheric evaporation, although it has nothing to do with the evaporation of any liquid. Initially cool material in the chromosphere is heated by downflowing, or precipitating, flare electrons that emit the hard X-rays and microwaves. The heated gas expands upward into the low-density corona along magnetic loops that, after filling, shine brightly in soft X-rays. When replenished and full, the post-impulsive flare loops contain plasma heated to temperatures of up to 40 million (4.0×10^7) degrees kelvin.

The soft X-rays emitted during solar flares are thermal radiation, released by virtue of the intense heat and dependent upon the random thermal motions of very hot electrons. At such high temperatures, the electrons are set free from atoms and move off at high speed, leaving the ions (primarily protons) behind. When a free electron moves through the surrounding material, it is attracted to the oppositely charged protons. The electron is therefore deflected from a straight path and changes its speed during its encounter with the proton, emitting electromagnetic radiation in the process (Fig. 6.6). This radiation is called *bremsstrahlung* from the German word for "braking radiation". Scientists use measurements of the flaring X-ray power to infer the density of the electrons emitting the bremsstrahlung (Focus 6.1).

Bremsstrahlung can be emitted at all wavelengths, from long radio waves to short X-rays, but during solar flares it becomes very intense at X-ray wavelengths. As we shall soon seen, the high-speed electrons accelerated during solar flares emit powerful radio-wavelength radiation by a different synchrotron process that involves electrons moving at nearly the velocity of light in the presence of magnetic fields. This radio synchrotron radiation is much more intense than the thermal bremsstrahlung at radio wavelengths during solar flares. In contrast, the free electrons in the outer quiescent, or non-flaring, solar corona do not move fast enough to emit synchrotron radiation, and they instead emit observable thermal bremsstrahlung at long radio wavelengths (Focus 5.4).

The hard X-rays marking the flare onset are also due to bremsstrahlung, but they are produced by electrons that have much higher energies than those emitting the thermal soft X-ray bremsstrahlung. These energetic, high-speed, non-thermal electrons are believed to be accelerated above the tops of coronal loops, and to radiate energy by non-thermal bremsstrahlung as they are beamed down along the looping magnetic channels into the low corona and chromosphere. Only about 0.000 01 or 10^{-5}, of the electron's energy is lost by this non-thermal bremsstrahlung; most of the energy is lost during collisions with ambient, non-flaring electrons.

Observations from the *Yohkoh* spacecraft, launched on 30 August 1991, have confirmed and extended this understanding of X-ray flares. They have shown exactly where both the soft X-rays and hard X-rays are coming from, and confirmed the overall Neupert effect/chromospheric evaporation scenario. According to this picture, solar flare energy release occurs mainly during the rapid, impulsive phase, when charged particles are accelerated and hard X-rays are emitted. The subsequent, gradual phase, detected by the slow build up of soft X-rays, is viewed as an atmospheric response to the energetic particles generated during the impulsive hard X-ray phase.

The *Yohkoh* spectrometer showed that the upflow of heated material coincides in time with the impulsive phase of flares detected as hard X-ray bursts and microwave bursts. *Yohkoh*'s Soft X-ray Telescope, or SXT, additionally demonstrated that the initial site of chromospheric evaporation coincides with the hard X-ray bursts at the footpoints of magnetic loops. Non-thermal electrons are apparently sent down along the closed magnetic loops into the initially low-temperature chromosphere, and the heated material subsequently expands upward to create the gradual soft X-ray phase seen in the corona.

Focus 6.1 Thermal electron density from soft X-ray bremsstrahlung

The greater the number of electrons, the stronger the thermal bremsstrahlung. To be precise, the thermal bremsstrahlung power, P, emitted from a plasma increases with the square of the electrons density, N_e, and the volume of the radiating source, V. It also depends upon the temperature of the electrons, T_e. A formula for the bremsstrahlung power is:

$$P = const \times N_e^2 \, V \, T_e^{1/2} \times \text{Gaunt factor},$$

where the Gaunt factor is also a function of the electron temperature. Scientists can use this expression with measurements of the X-ray power during a flare to determine the density of electrons participating in the radiation, assuming that they completely fill the observed volume. Electron density values of $N_e \approx 10^{17}$ electrons per cubic meter are often obtained. Densities of 10^{17} to 10^{18} electrons per cubic meter have also been derived from the ratios of density-sensitive soft X-ray emission lines detected during solar flares.

Fig. 6.7 **Double hard X-ray sources** Hard X-ray flares often appear as double sources that are aligned with the photosphere footpoints of a flaring magnetic loop detected at soft X-ray wavelengths. These footpoints can also be the sites of white-light flare emission. The time profiles of this flare, detected on 15 November 1991, show that the increase of white-light emission matches almost exactly that of the hard X-ray flux. This and the simultaneity of hard X-ray emission from the two footpoints establish that non-thermal electrons transport the impulsive-phase energy along the flare loops. These soft X-ray, hard X-ray and white-light images of the solar flare were taken with telescopes aboard the *Yohkoh* mission. (Courtesy of NASA, ISAS, the Lockheed-Martin Solar and Astrophysics Laboratory, the National Astronomical Observatory of Japan, and the University of Tokyo.)

With *Yohkoh*, the double-source, loop footpoint structure of impulsive hard X-ray flares was confirmed with unprecedented clarity. It established a double-source structure for the hard X-ray emission of roughly half the flares observed in the purely non-thermal energy range above 30 keV. The other half of the flares detected with *Yohkoh* were either single sources, that could be double ones that are too small to be resolved, or multiple sources that could be an ensemble of double sources. As subsequently discussed (Section 6.3), a third hard X-ray source is sometimes detected near the apex of the magnetic loop joining the other two; this loop-top region marks the primary energy release site and the location of electron acceleration due to magnetic interaction.

Two white-light emission patches were also detected by *Yohkoh* during at least one flare, at the same time and place as the hard X-ray sources (Fig. 6.7). This shows that the rarely-seen, white-light flares can also be produced by the downward impact of non-thermal electrons, and demonstrates their penetration deep into the chromosphere.

Flare-accelerated ions are also hurled down into the lower solar atmosphere, generating gamma rays there. Gamma rays are even more energetic than X-rays, exceeding 100 keV in energy. The hard X-ray and gamma-ray time profiles of solar flares are time-coincident within the accuracy of measurement, demonstrating the simultaneous acceleration of relativistic electrons and energetic ions in solar flares to within a few seconds. Measurements of the high-energy electrons are obtained from the hard X-rays, produced by non-thermal bremsstrahlung during solar flares, and the flare-accelerated ions are observed using gamma rays. In large solar flares, the onset of the impulsive phase emission is simultaneous for radiation with energies from about 40 keV (hard X-rays) to about 40 MeV (gamma rays). This provides important constraints to theories for how particles are accelerated in solar flares.

Gamma rays from solar flares

Protons and heavier ions are accelerated to high speed during solar flares, and beamed down into the chromosphere where they produce nuclear reactions and generate gamma rays, the most energetic kind of radiation detected from solar flares. Thus, for a few minutes, during an impulsive phase of a solar flare, nuclear reactions occur in the low, dense solar atmosphere; they also occur all the time deep down in the Sun's energy-generating core that is even denser and hotter. Like X-rays, the gamma rays are totally absorbed in our air and must be observed from space.

The protons slam into the dense, lower atmosphere, like a

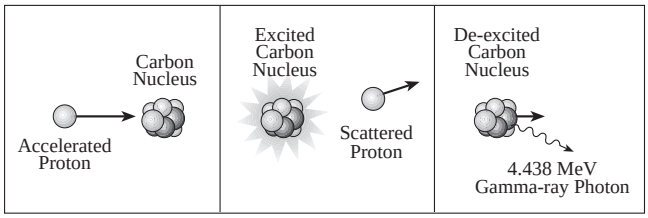

Figure 6.8 **Gamma rays during solar flares** Energetic protons, accelerated during solar flares, can encounter the nuclei of carbon and other elements found in the solar atmosphere. The nucleus is excited to a higher energy level during each collision. It then emits gamma radiation (called a gamma-ray photon) with a specific energy characteristic of the nucleus involved.

bullet hitting a concrete wall, shattering nuclei in a process called spallation. The nuclear fragments are initially excited, but then relax to their former state by emitting gamma rays (Focus 6.2). Other abundant nuclei are energized by collision with the flare-accelerated protons, and emit gamma rays to get rid of the excess energy (Fig. 6.8). The excited nuclei emit gamma rays during solar flares at specific, well-defined energies between 0.4 and 7.1 MeV. One MeV is equivalent to a thousand keV and a million electron volts, so the gamma rays are ten to one hundred times more energetic than the hard X-rays and soft X-rays detected during solar flares.

During bombardment by flare-accelerated ions, energetic neutrons can be torn out of the nuclei of atoms. Whenever one of these neutrons is eventually captured by a hydrogen nucleus (proton) in the photosphere, the neutron and proton form a deuteron nucleus, D, with the delayed emission of a gamma ray line at 2.223 MeV. It is typically the strongest gamma-ray line in solar flare spectra.

Particles of anti-matter are also produced during solar flares, in the form of positrons, e^+, but they cannot stay around very long in our material world. The positrons almost instantaneously annihilate with their material counterparts, the electrons denoted by e^-, producing radiation at 0.511 MeV. It is the second-strongest-gamma ray line from solar flares.

Narrow gamma-ray lines (≤ 100 keV in width) have been observed during solar flares from deuteron formation, or neutron capture, electron-positron annihilation, and excited carbon, nitrogen, oxygen and heavier nuclei (Table 6.3), mainly in the 1980s using the Gamma Ray Spectrometer (GRS) aboard the *Solar Maximum Mission* (*SMM*) satellite.

When protons with energies above 300 MeV interact with the abundant hydrogen in the solar atmosphere, they can produce short-lived fundamental particles, called mesons, whose decay also leads to gamma-ray emission. The decay of neutral mesons produces a broad gamma-ray peak at 70 MeV, but the decay of charged mesons leads to bremsstrahlung giving a continuum of gamma rays with energies extending to several MeV.

Neutrons with energies above 1000 MeV can also be produced during solar flares. Such energetic neutrons have been directly measured in space near Earth in the 1980s from the *SMM* and in the 1990s from the *Compton Gamma Ray Observatory*. In the most energetic flares showing meson decay gamma-ray emission, the associated relativistic neutrons can reach the Earth and produce a signal in ground-level neutron monitors.

Non-thermal electrons that have been accelerated during solar flares are additionally hurled out into interplanetary space, emitting intense radio emission in the process. The

Element	Energy (MeV)	Element	Energy (MeV)
Delayed lines		*Proton excitation*	
$e^+ + e^-$ (positron and electron) (pair annihilation)	0.511*	^{14}N (nitrogen)	5.105* 2.313
^{2}H (= D) (deuterium) (neutron capture)	2.223*	^{20}Ne (neon)	1.634* 2.613 3.34
Spallation			
^{12}C (carbon) ^{16}O (oxygen)	4.438* 6.129* 6.917* 7.117* 2.741	^{24}Mg (magnesium)	1.369* 2.754
		^{28}Si (silicon)	1.779* 6.878
Alpha Excitation		^{56}Fe (iron)	0.847* 1.238* 1.811
^{7}Be (beryllium) ^{7}Li (lithium)	0.431* 0.478*		

[a] The most-prominent lines are marked with an asterisk * and have been detected in the flare of 27 April 1981. The energy is given in MeV, where 1 MeV = 1000 keV = 1.6022×10^{-13} J or 1.6022×10^{-6} erg.

Table 6.3 **Some important gamma-ray lines from solar flares**[a]

Focus 6.2 Nuclear reactions on the Sun

Nuclear reactions during solar flares produce gamma-ray lines, emitted at energies between 0.4 and 7.1 MeV. They result when either flare-accelerated protons or flare-accelerated helium nuclei, known as alpha particles, collide with nuclei in the dense atmosphere below the acceleration site.

These reactions are often written using letters to denote the nuclei, a Greek letter γ to denote gamma-ray radiation, and an arrow $\rightarrow$ to specify the reaction; nuclei on the left side of the arrow react to form products given on the right side of the arrow. The letter p is used to denote a proton, the nucleus of a hydrogen atom, and the Greek letter α signifies an alpha particle, which is the nucleus of the helium atom.

The collision of a flare-associated proton, p, or alpha particle, α, with a heavy nucleus in the dense solar atmosphere may result in a spallation reaction that causes the nucleus to break up into lighter fragments that are left in excited states denoted by an asterisk *. They subsequently de-excite to emit gamma-ray lines. For example, the collision of a flaring proton, p, with an oxygen, ^{16}O, or a neon, ^{20}Ne, nucleus produces excited carbon, $^{12}C^*$, and oxygen, $^{16}O^*$, by the reactions:

$$p + {}^{16}O \rightarrow {}^{12}C^* + \alpha$$

and

$$p + {}^{20}Ne \rightarrow {}^{16}O^* + \alpha,$$

with de-excitation and emission of a gamma-ray line, γ, of energy, $h\nu$, by:

$${}^{12}C^* \rightarrow {}^{12}C + \gamma \qquad (h\nu = 4.438 \text{ MeV})$$

and

$${}^{16}O^* \rightarrow {}^{16}O + g \qquad (h\nu = 6.129 \text{ MeV}).$$

A flare-accelerated proton, p, can bounce off nucleus, N, one of the abundant nuclei in the solar atmosphere, exciting it by the reaction:

$$N + p \rightarrow N^* + p'$$

where the unprimed and primed sides respectively denote the incident and scattered proton, p. The excited nucleus N* reverts to its former unexcited state by emitting a gamma-ray line, γ, in a reaction denoted by:

$$N^* \rightarrow N + \gamma.$$

Elements and energies of prominent gamma-ray lines resulting from proton excitation of abundant solar elements are given in Table 6.3.

Heavy excited nuclei can also be generated by the fusion of flare-associated particles with lighter nuclei in the atmosphere. Examples include beryllium, $^7Be^*$, and lithium, $^7Li^*$, produced by flaring alpha particles, α, and ambient helium, ^4He.

$$\alpha + {}^4He \rightarrow {}^7Be^* + n$$

and

$$\alpha + {}^4He \rightarrow 7Li^* + p\,,$$

with the excited nuclei emitting a gamma-ray line, γ, of energy, $h\nu$, by de-excitation:

$${}^7Be^* \rightarrow {}^7Be + \gamma \qquad (h\nu = 0.431 \text{ MeV})$$

and

$${}^7Li^* \rightarrow {}^7Li + \gamma \qquad (h\nu = 0.478 \text{ MeV}).$$

Gamma-ray lines are produced at 0.511 MeV when matter and anti-matter annihilate each other during solar flares, disappearing in a puff of radiation by:

$$e^- + e^+ \rightarrow \gamma + \gamma \qquad (h\nu = 0.511 \text{ MeV}),$$

where e^- and e^+ respectively denote an electron and a positron.

Another common gamma-ray line is the feature at 2.223 MeV associated with neutron, n, capture by hydrogen nuclei, ^1H, to produce excited deuterons, or excited deuterium nuclei denoted by $^2H^*$, that relax with the emission of gamma rays, γ.

$${}^1H + n \rightarrow {}^2H^*$$

with

$${}^2H^* \rightarrow {}^2H + \gamma \qquad (h\nu = 2.223 \text{ MeV}).$$

The neutrons are produced when flare-associated ions hit atmospheric nuclei and break them apart. The neutron-capture line emission is delayed, typically by one hundred seconds, from the time of flare acceleration since the neutrons must adjust, or thermalize, before they are captured by the abundant hydrogen nuclei in the photosphere.

expulsion of these energetic electrons has been confirmed by direct *in-situ* measurements in interplanetary space (Section 7.1, Fig. 7.1).

Solar radio bursts

The radio emission of a solar flare is often called a radio burst to emphasize its brief, energetic and explosive characteristics. During such outbursts, the Sun's radio emission can increase up to a million times normal intensity in just a few seconds, so a solar flare can outshine the entire Sun at radio wavelengths. Although the radio emission of a solar flare is much less energetic than the flaring X-ray emission, the solar radio bursts provide an important diagnostic tool for specifying the magnetic and temperature structures at the time. They additionally provide evidence for electrons accelerated to very high speeds, approaching that of light, as well as powerful shock waves.

Radio bursts do not occur simultaneously at different radio frequencies, but instead drift to later arrival times at lower frequencies. This is explained by a disturbance that travels out through the progressively more rarefied layers of the solar atmosphere, making the local electrons in the corona vibrate at their natural frequency of oscillation, called the plasma frequency (Focus 6.3).

Australian radio astronomers pioneered this type of

Focus 6.3 Exciting plasma oscillations in the corona

At the high million-degree temperature of the solar corona, electrons are stripped from abundant hydrogen atoms by innumerable collisions, leaving electrons and protons that are free to move about. The electrons have a negative charge, and the protons are positively charged by an equal amount. The mixture of electrons and protons in the solar corona is called a plasma, and it has no net charge.

When a flare-associated disturbance, such as an electron beam or a shock wave, moves though the coronal plasma, the local electrons are displaced with respect to the protons, which are more massive than the electrons. The electrical attraction between the electrons and protons pulls the electrons back in the opposite direction, but they overshoot the equilibrium position. The light, free electrons therefore oscillate back and forth when a moving disturbance passes through the corona.

The natural frequency of oscillation, called the plasma frequency, depends on the local electron concentration, with a lower plasma frequency at smaller coronal electron densities. The plasma frequency therefore decreases with diminishing electron density at greater distances from the Sun. The exact expression for the plasma frequency, ν_p, is:

$$\nu_p = \left[\frac{e^2 N_e}{4\pi^2 \varepsilon_0 m_e}\right]^{1/2} = [81 N_e]^{1/2} \text{ Hz}$$

where the electron density, denoted by N_e, is in units of electrons per cubic meter, the electron charge $e = 1.6022 \times 10^{-19}$ coulomb, the electron mass $m_e = 9.1094 \times 10^{-31}$ kg, the constant $\pi = 3.141\,59$, and the permittivity of free space $\varepsilon_0 = 10^{-9}/(36\pi)$ farad m^{-1}.

Low in the solar corona, where $N_e \approx 10^{14}$ m^{-3}, the plasma frequency is $\nu_p \approx 9 \times 10^7$ Hz = 90 MHz, where one MHz is a million Hz or a million cycles per second. The product of frequency and wavelength is equal to the velocity of light $c = 2.9979 \times 10^8$ m per second, so a frequency of 90 MHz corresponds to a wavelength of 3.33 m. Thus, a solar flare can set the corona oscillating at radio wavelengths of a few meters and less.

As the explosive disturbance moves out through the progressively more rarefied layers of the corona, it excites radiation at lower and lower radio frequencies. Ground-based radio telescopes can identify these radio signals by changing the frequency to which their receiver is tuned. As an example, the radiation at a frequency of 200 MHz, or at 1.5-m wavelength, might arrive about a minute before the 20 MHz (15 m) outburst.

With an electron density model of the solar atmosphere (Fig. 6.9), the emission frequency can be related to height, and combined with the time delays between frequencies to obtain the outward velocity of the moving disturbance. Electron beams that produce type III radio bursts (Table 6.4) are moving at velocities of up to half the velocity of light, or 150 million meters per second. Outward moving shock waves that generate type II radio bursts move at a slower speed, at about a million meters per second.

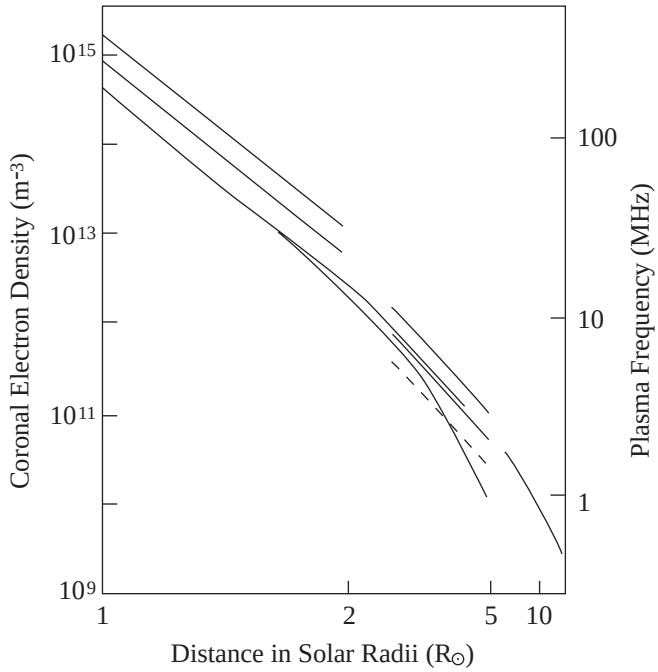

Fig. 6.9 **Plasma frequency and coronal electron density** The plasma frequency (*right axis*) that corresponds with the electron density (*left axis*) in the corona, as inferred from measurements during total eclipses of the Sun. The dashed line is for a coronal hole. As the corona expands out to larger distances from the Sun, and into an ever-larger volume of space, it becomes thinner and less dense, and the plasma frequency is smaller.

investigation in the 1950s, using swept-frequency receivers to distinguish at least two kinds of meter-wavelength radio bursts (Table 6.4). Designated as type II and type III bursts, they both show a drift from higher to lower frequencies, but at different rates. The most common bursts detected at meter wavelengths are the fast-drift type III bursts that provide evidence for the ejection of very energetic electrons from the Sun, with energies of about 100 keV. (An electron moving at half the velocity of light, c, has a kinetic energy of $0.5\ m_e V^2 = 1.6022 \times 10^{-14}$ J or 100 keV, where m_e is the mass of the electon and the velocity $V = 0.5\ c$.) These radio bursts last for only a few minutes at the very onset of solar flares and extend over a wide range of radio frequencies (Fig. 6.10).

The slow-drift type II radio bursts drift to lower frequencies at a leisurely pace, corresponding to an outward velocity of about a million meters per second. They are excited by shock waves set up at the time of a solar explosion and moving out into space. Spatially-resolved radio interferometric observations indicate that the type II bursts are very large, with angular extents that can become comparable to that of the Sun.

Solar radio astronomers usually measure frequency in units of MHz, where 1 MHz is equal to a million, or 10^6, Hz. A frequency of 300 MHz corresponds to a wavelength of 1 m. Ground-based instruments observe the dynamic spectra, or frequency drift, for solar radio bursts between 10 MHz and 8000 MHz. Solar radiation is reflected by the Earth's ionosphere at frequencies below 10 MHz, or wavelengths longer than 30 m, and cannot reach the ground.

Type I bursts (Noise storms)	Long-lived (hours to days) sources of radio emission with brightness temperatures from ten million to a billion (10^7 to 10^9) degrees kelvin. Although noise storms are the most common type of activity observed on the Sun at meter wavelengths, they are not associated with solar flares. Noise storms are attributed to electrons accelerated to modest energies of a few keV within large-scale magnetic loops that connect active regions to more distant areas of the Sun.
Type II bursts	Meter-wavelength type II bursts have been observed at frequencies between 0.1 and 100 MHz. A slow drift to lower frequencies at a rate of about 1 MHz per second suggests an outward motion at about a million meters per second and has been attributed to shock waves.
Type III bursts	The most common flare-associated radio bursts at meter wavelengths, observed from 0.1 to 1000 MHz. Type III bursts are characterized by a fast drift from high to low frequency, at a rate of up to 100 MHz per second. They are attributed to beams of electrons thrown out from the Sun with kinetic energies of 10 to 100 keV, and velocities of up to half the velocity of light, or 150 million meters per second. The U-type bursts are a variant of type III bursts that first decrease in frequency and then increase again, indicating upward and downward electron motion along closed magnetic field lines.
Type IV bursts	Broad-band continuum radiation lasting for up to one hour after impulsive flare onset. The radiation from a moving type IV burst is partly circularly polarized, and has been attributed to synchrotron emission from energetic electrons trapped within magnetic clouds that travel out into space with velocities from several hundred thousand to a million meters per second.
Centimeter bursts	Impulsive continuum radiation at centimeter wavelengths that lasts just a few minutes. These microwave bursts are attributed to the gyrosynchrotron radiation of high-speed electrons accelerated to energies of 100 to 1000 keV. The site of acceleration is located above the tops of coronal loops.
Millisecond spikes	Radio flares can include literally thousands of spikes, each lasting a few milliseconds, suggesting sizes less than a million meters across and brightness temperatures of up to a million billion (10^{15}) degrees kelvin, requiring a coherent radiation mechanism.

[a]A frequency of one MHz corresponds to a million Hz, or 10^6 Hz. An energy of 1 keV corresponds to 1.6022×10^{-16} J or 1.6022×10^{-9} erg.

Table 6.4 **Types of solar radio bursts**[a]

Terrestrial long-wavelength radio communication utilizes this reflective capability of the ionosphere to get around the curvature of the Earth.

Spacecraft lofted above the ionosphere are used to track high-speed electrons or shock waves at remote distances from the Sun, where the density and plasma frequency are low. They have monitored the corona's plasma radiation at frequencies from 0.01 to 10 MHz for more than three decades (see Section 7.1, Fig. 7.1).

A type III radio burst emits non-thermal radiation, and cannot be due to the thermal radiation of a hot gas. Thermal radiation is emitted by a collection of particles that collide with each other and exchange energy frequently, giving a distribution of particle energy that can be characterized by a single temperature. Impulsive solar flares do not have enough time to achieve this equilibrium, and the flaring electrons are far too energetic for a thermal process to be at work. To make electrons travel at half the speed of light, with a kinetic energy of 100 keV, a thermal gas would have to be heated to implausible temperatures of one billion degrees, or about 70 times hotter than the center of the Sun. The non-thermal radio bursts are instead accelerated by different

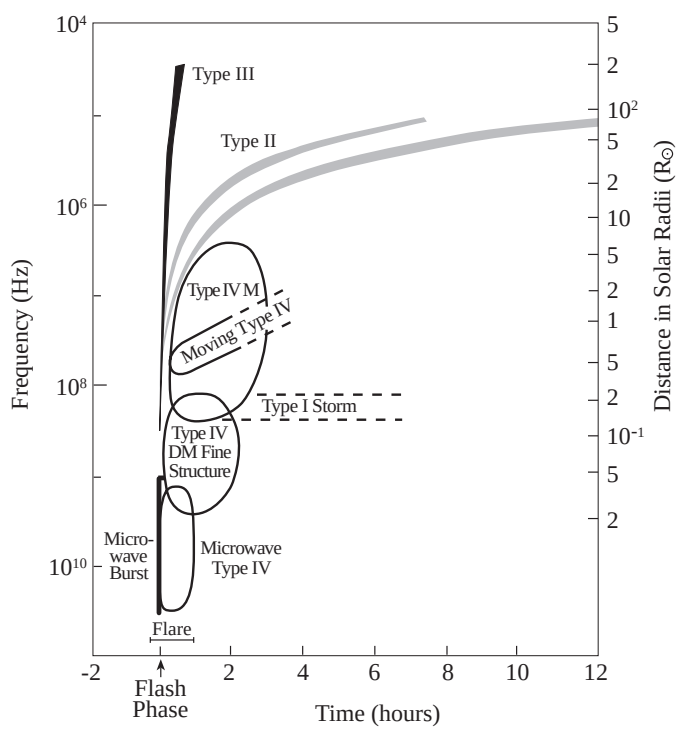

Fig. 6.10 **Solar radio bursts** A large solar flare can be associated with several different kinds of intense radio emission, depending on the frequency (*left vertical axis*) and time after the explosion (*bottom axis*). The impulsive, or flash, phase of the solar flare, starting at 0 hours, normally lasts about 10 minutes and is associated with a powerful microwave burst. Dynamic spectra at frequencies of about 10^8 Hz, show type II and type III bursts that drift from high to low frequencies as time goes on, but at different rates depending on the type of burst. The distance scale (*right vertical axis*) is in units of the Sun's radius of 696 million meters; it is the distance at which the coronal electron density yields a plasma frequency corresponding to the frequency on the left-hand side.

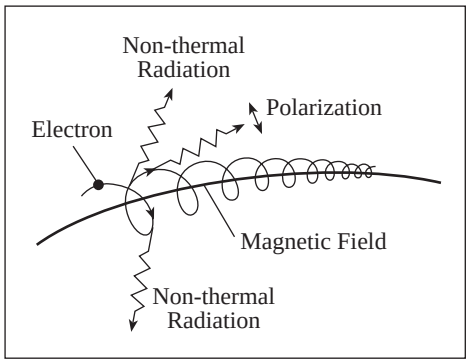

Fig. 6.11 **Synchrotron radiation** High-speed electrons moving at velocities near that of light emit a narrow beam of synchrotron radiation as they spiral around a magnetic field. This emission is sometimes called non-thermal radiation because the electron speeds are much greater than those of thermal motion at any plausible temperature. The name "synchrotron" refers to the man-made, ring-shaped synchrotron particle accelerator where this type of radiation was first observed; a synchronous mechanism keeps the particles in step with the acceleration as they circulate in the ring.

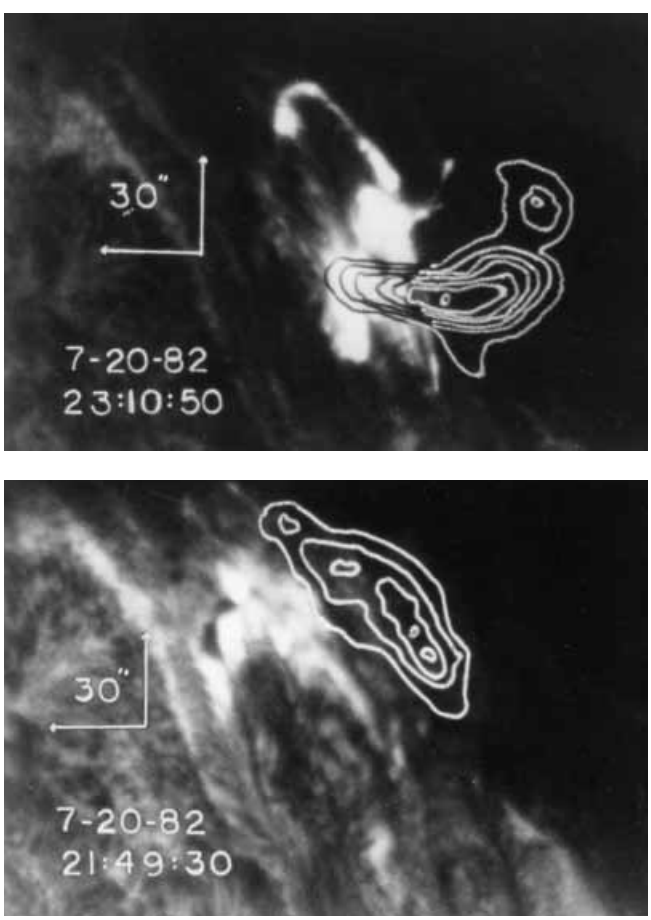

Fig. 6.12 **Site of radio burst** Electrons are rapidly accelerated just above the tops of coronal loops during the early stages of the flare, emitting the powerful loop-like radio signals mapped here with white contours. The underlying hydrogen-alpha (Hα) emission is shown in the accompanying photographs. These 10-second snapshot radio maps were obtained with the Very Large Array (VLA) at a wavelength of 20 cm, or a frequency of 1420 MHz. The angular extent of each 20-cm flaring loop is about one minute of arc, or one-thirtieth of the angular width of the visible solar disk.

processes.

Other non-thermal radio outbursts associated with solar flares, and designated type IV bursts, were discovered at the Nancay Observatory in France. The best-studied component is the so-called moving type IV bursts observed at frequencies from roughly 10 MHz to 100 MHz. They are explained by energetic electrons trapped in a magnetic cloud that is propelled outward into the solar atmosphere at a speed of 10^5 to 10^6 m s^{-1}. Like the non-thermal electrons that produce type III bursts, the electrons giving rise to type IV bursts are traveling at speeds far exceeding those of thermal motions at any plausible temperature.

Focus 6.4 Coherent radio bursts from the Sun and other active stars

Radio astronomers use brightness temperature, T_B, to quantify the emission from radio sources. For a source of radius, R, distance, D, and radio flux density, S, at wavelength, λ, we have $T_B = S\lambda^2D^2/(2\pi kR^2)$, where k is Boltzmann's constant (Focus 5.4). The brightness temperature is that temperature the source would have if it was emitting thermal radiation from a hot gas. For a given flux density, wavelength and distance, a smaller source has a higher brightness temperature.

Exceptionally small sizes, and correspondingly high brightness temperatures, are inferred for very rapid radio bursts on the Sun and other active stars. In some extreme instances, solar flares at decimeter wavelengths include radio spikes with a rapid rise as short as a few milliseconds and similarly brief duration. Since nothing can move faster than the velocity of light, it sets an upper limit on any travel-time. Rapid changes over time-scales of a few milliseconds therefore restrict the size of the radiating volume to relatively small spatial scales of less than a few million meters across. The radio spikes must have brightness temperatures as high as a million billion (10^{15}) degrees kelvin if their intense radiation is emitted from such a small source.

Yet, such high temperatures on the Sun or other active stars are impossible to achieve by heating any gas, and have only been realized in the earliest, big-bang stages of the expanding Universe where material particles, as we know them, did not exit. The high brightness temperatures of millisecond radio spikes are explained by coherent radiation of ordinary particles working together in an organized manner, rather than by the random, incoherent motions of heated gas particles.

Rapid radio flares from dwarf M stars require sources much smaller than the visible stars in size, implying brightness temperatures exceeding 10^{15} K, so they also require a coherent radiation mechanism. The high circular polarization (100 percent) of these stellar radio bursts indicates an intimate connection with stellar magnetic fields. The available radio and X-ray evidence for flares on other late type stars, including RS CVn binaries, suggests that they also have highly structured magnetic coronas with active regions that are much smaller than the visible stars, and coherent non-thermal radio bursts.

The high-speed electrons that emit type III or type IV bursts spiral around the magnetic field lines in the low corona, moving rapidly at velocities near that of light, and send out radio waves called synchrotron radiation after the man-made synchrotron particle accelerator where it was first observed (Fig. 6.11). Unlike the thermal radiation of a very hot gas, the non-thermal synchrotron radiation is most intense at long, invisible radio wavelengths rather than short X-rays.

Radio bursts at meter wavelengths occur at altitudes far above the site where the flare energy is released and particles are accelerated. The high-speed electrons originate much lower in the corona, and are observed at decimeter-wavelengths (1 decimeter = 0.1 meter = 10 centimeter). Decimeter-wavelength bursts have been observed by Swiss radio astronomers at frequencies up to 8000 MHz, and at wavelengths as short as 3.75 centimeters, moving downward from the acceleration regions into the low corona.

A giant array of radio telescopes, located near Socorro, New Mexico and called the Very Large Array (Section 9.2), can zoom in at the very moment of a solar flare, taking snapshot images with just a few seconds exposure (Fig. 6.12). It has pinpointed the location of the impulsive decimeter radiation and the electrons that produce it. These radio bursts are triggered low in the Sun's atmosphere, unleashing their vast power just above the apex of magnetic arches, called coronal loops, that link underlying sunspots of opposite magnetic polarity. Some of the energetic electrons are confined within the closed magnetic structures, and are forced to follow the magnetic fields down into the chromosphere. Other high-speed electrons break free of their magnetic cage, moving outward into interplanetary space along open magnetic field lines and exciting the meter-wavelength type III bursts.

To complete our inventory of solar radio bursts, there are millisecond spikes whose rapid rise times and short duration require an entirely different, coherent radiation mechanism that is also needed to explain some radio bursts on other active stars (Focus 6.4).

6.2 Coronal mass ejections and eruptive prominences

Another dramatic, magnetically energized type of solar explosion is called a Coronal Mass Ejection, or CME for short. This is a giant magnetic bubble that rapidly expands to rival the Sun in size, and hurls billions of tons of million-degree gas into interplanetary space at speeds of about 4×10^5 m s^{-1}, reaching the Earth in about four days. Their associated shocks accelerate and propel vast quantities of high-speed particles ahead of them.

CMEs are detected during routine visible-light observations of the corona from spacecraft such the *SOlar and Heliospheric Observatory*, or *SOHO*. With a disk in the center to block out the Sun's glare, the coronagraph sees huge pieces of the corona that are blasted out from the edge of the occulted photosphere (Figs. 6.13, 6.14). The mass ejections are seen as bright moving loop-like features in the corona, whose white light is scattered by free electrons.

Bright regions in coronagraph images have the greatest concentration of electrons and therefore contain excess coronal mass, while dark regions have fewer electrons and less mass. Each time a mass ejection rises out of the corona, it carries away 5 to 50 billion tons (5×10^{12} to 5×10^{13} kg) of coronal material. A CME therefore rips a giant piece out of the corona, and this causes a scar-like reduction in its soft X-ray emission. The expelled mass inferred from this large-scale, soft X-ray dimming of the soft X-ray corona is comparable to that estimated for coronal mass ejections (see Focus 6.5).

Coronal mass ejections are huge. Their average angular span of 45 degrees along the disk edge implies a size near the Sun that is comparable to that of the visible solar disk, and they can expand to even larger sizes further out.

Nearly everything we know about CMEs has been learned in just a few decades. They were discovered on 14 December 1971 and 8 Februrary 1972 using the white-light coronagraph aboard NASA's *Seventh Orbiting Solar Observatory* (*OSO 7*). Since then, thousands of CMEs have been identified

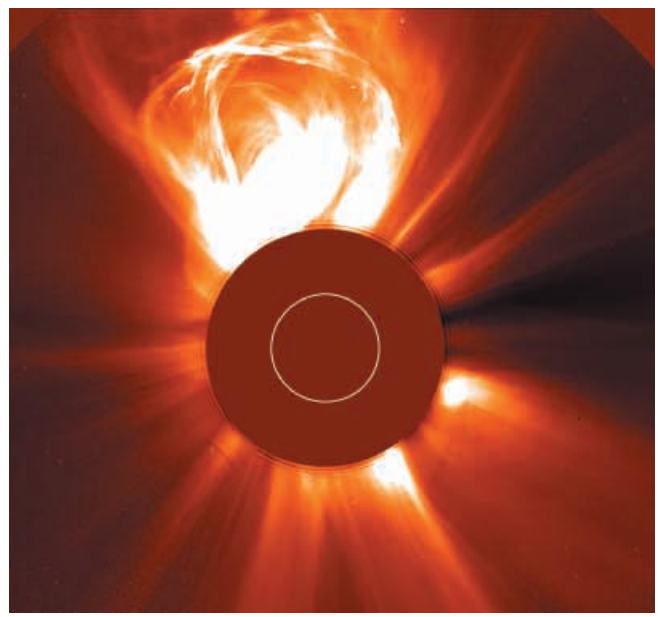

Fig. 6.13 **Coronal mass ejection** A huge coronal mass ejection is seen in this coronagraph image, taken on 27 February 2000 with the Large Angle Spectrometric COronagraph (LASCO) on *SOHO*. The white circle denotes the edge of the photosphere, so this mass ejection is about twice as large as the visible Sun. The dark area corresponds to the occulting disk of the coronagraph that blocks intense sunlight and permits the corona to be seen. About one hour before this image was taken, another *SOHO* instrument, the Extreme-ultraviolet Imaging Telescope or EIT, detected a filament eruption lower down near the solar chromosphere. (Courtesy of the *SOHO* LASCO consortium. *SOHO* is a project of international cooperation between ESA and NASA.)

Satellite	OSO 7	*Skylab*	P78-1	SMM	SOHO
Coronagraph		ATM[a]	Solwind	C/P[b]	LASCO/C3[c]
Observation time	Oct. 71 to June 74	May 73 to Feb. 74	March 79 to Sept. 85	Feb.–Sept. 80 Apr. 84 to Nov. 89	Feb. 96 on
Field of view[d]	3 to 10 $R_\odot$	1.6 to 6 $R_\odot$	2.6 to 10 $R_\odot$	1.6 to 8 $R_\odot$	3.7 to 30 $R_\odot$
Resolution[e] (seconds of arc)	75	8	75	6.4	56

[a] Apollo Telescope Mount; [b] designates Coronagraph/Polarimeter; [c] LASCO consists of three coronagraphs, designated C1, C2 and C3, with respective overlapping fields of view of 1.1 to 3, 1.7 to 6, and 3.7 to 32 solar radii and respective pixel angular resolutions of 5.6, 11.2 and 56.0 seconds of arc; [d] here $R_\odot$ denotes the solar radius, or 696 million (6.96×10^8) meters; [e] an angular resolution of 1 second of arc corresponds to 725 thousand (7.25×10^5) meters at the Sun.

Table 6.5 **Space-borne orbiting coronagraphs**[a]

using data from the NASA's *Skylab* in 1973-74, the U. S. Air Force's P78-1 satellite (1979-1985), NASA's *Solar Maximum Mission* (SMM, 1980 and 1984-1989), and the Large Angle Spectrometric COronagraph (LASCO) of the *SOlar and Heliospheric Observatory* (SOHO, 1996 on) – Table 6.5. LASCO observes the corona from 1.1 to 30 solar radii from Sun center, looking closer to, and further from, the Sun than all previous space-borne coronagraphs.

These spacecraft observations have established the essential physical properties of coronal mass ejections, showing that they are big, massive, fast and energetic (Table 6.6).

The Sun is not wasting away because of coronal mass ejections, in spite of their awesome mass. Coronal mass ejections typically occur only once a day, on average, and therefore account for only about five percent of the mass loss due to the steady, perpetual solar wind (Focus 6.5).

By the time that they are a few solar radii above the photosphere, CMEs have reached a cruising velocity of about 4×10^5 m s^{-1}. At that speed, the expelled mass can reach the Earth in about 100 hours, carrying with it an average kinetic energy of 10^{23} to 10^{24} J (Focus 6.5). The amount of energy that a CME liberates in producing the motions of the expelled mass and in lifting it against the Sun's powerful gravity is roughly comparable to the energy of a typical solar flare. However, most of the energy of a mass ejection goes into the expelled material, while a flare's energy is mainly transferred into accelerated particles that subsequently emit intense X-ray and radio radiation.

Since the white-light brightness varies in proportion to the electron density and does not depend on the temperature, the coronagraph images reveal the density structure of the corona. Sequential coronagraph images record changes in the density of the corona, and thereby reveal transient expulsions of matter at the apparent edge of the Sun. These CMEs balloon out of the solar atmosphere at high speed, moving through the coronagraph's field of view in just a few hours. Such events work only in one direction, always moving away from the Sun into interplanetary space and never falling back in the reverse direction.

Coronal mass ejections usually have expanding

Characteristic	*Value*
Average angular width (heliocentric)	45 degrees
Largest mass ejected	5×10^{12} to 5×10^{13} kg (5 to 50 billion tons)
Frequency of occurrence [b]	3.5 events per day (activity maximum) 0.2 events per day (activity minimum)
Mass flow rate	About 2×10^8 kilograms per second
Speed range of leading edge	5×10^4 to 1.2×10^6 m s^{-1}
Average speed of leading edge	4×10^5 m s^{-1}
Average time to reach Earth	About 100 hours
Average kinetic energy	Approximately 10^{23} to 10^{24} J

[a] Also see Focus 6.5.
[b] LASCO's improved sensitivity enabled it to detect 0.8 events per day during activity minimum.

Table 6.6 **Physical properties of coronal mass ejections near the Sun**[a]

Focus 6.5 Mass, mass flux, energy and time delay of coronal mass ejections

Coronal mass ejections are detected as localized increases in the brightness of white-light coronagraph images. Integration of the brightness increase, that depends only on the electron density, N_e, permits evaluation of the total mass, M, of the ejection. For a sphere of radius, R, we have:

$$M = 4\pi R^3 N_e m_p /3,$$

where the proton mass $m_p = 1.67 \times 10^{-27}$ kg. The corona is a fully ionized, predominantly (90 percent) hydrogen plasma, so the number densities of protons and electrons are equal, but since the protons are 1,836 times more massive than the electrons, the protons dominate the mass.

For a mass ejection with an electron, or proton, density of $N_e = 10^{13}$ electrons per cubic meter, that has grown as large as the Sun, with $R = 6.96 \times 10^8$ m, this expression gives

$$M = 10^{13} \text{ kg} = 10 \text{ billion tons},$$

where one ton is equivalent to 1000 kilograms. Because it looks at regions further away from the Sun than previous coronagraphs were able to do, the LASCO coronagraph observes CMEs that sometimes evolve into bigger structures than those seen before, leading to mass estimates up to 50 billion tons.

At the rate of one ejection per day, and 10^{13} kg per ejection, this amounts to a mass flow rate of about 10^8 kg s^{-1}, since there are 86 400 seconds per day. By way of comparison, the flux of the solar wind, discussed in the next chapter, is about 5×10^{12} protons m^{-2} s^{-1}, or 8.3×10^{-15} kg m^{-2} s^{-1} near the Earth. If this flux is typical of that over the entire Sun-centered sphere, with an average Sun-Earth distance of $D = 1.5 \times 10^{11}$ m, we can multiply by the sphere's surface area, $4\pi D^2$, to obtain a solar-wind mass flux of about 2×10^9 kg s^{-1}. Thus, coronal mass ejections contribute roughly five percent of the solar-wind mass flux.

The kinetic energy of a coronal mass ejection with a speed of $V = 4 \times 10^5$ m s^{-1} and a mass $M = 10^{13}$ kg is:

$$\text{kinetic energy} = MV^2/2 \approx 10^{24} \text{ J} = 10^{31} \text{ erg}.$$

This is comparable to the energies of large solar flares that lie between 10^{21} and 10^{25} J.

At a speed of $V = 4 \times 10^5$ m s^{-1}, the time, T, to travel the average distance, D, from the Sun to the Earth is:

$$T = D/V = 3.75 \times 10^5 \text{ s} = 104 \text{ hours} = 4.34 \text{ days}.$$

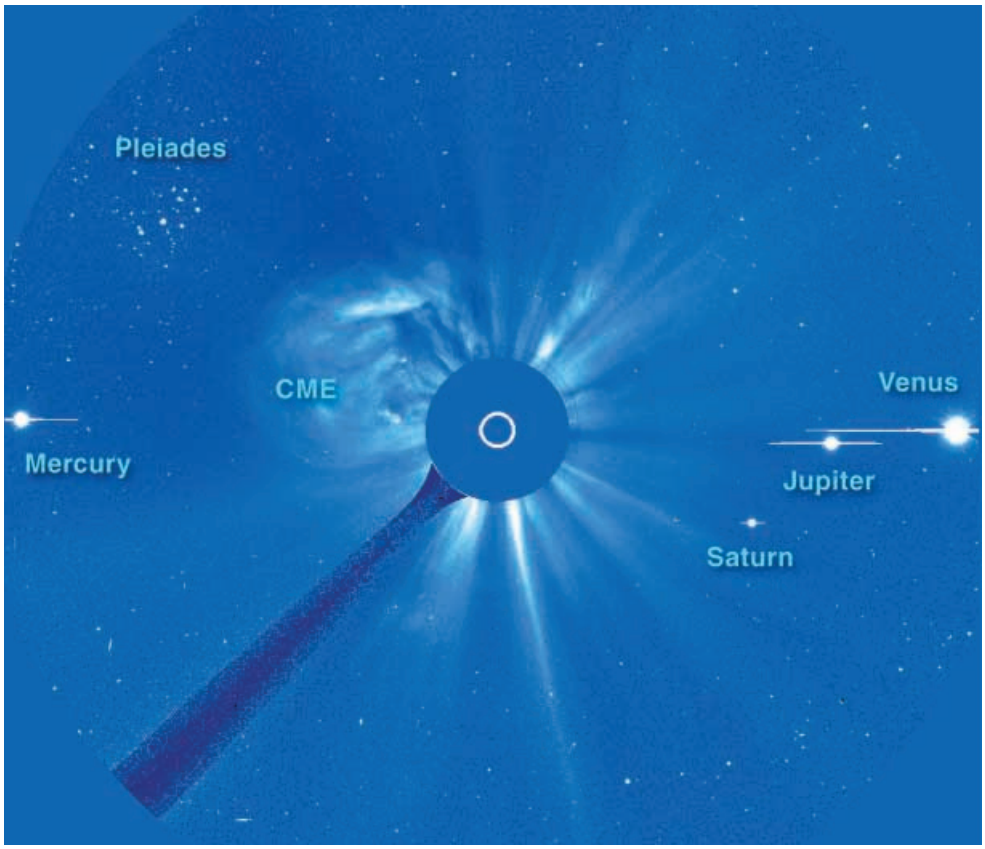

Fig. 6.14 **Coronal mass ejection, planets and Pleiades** A Coronal Mass Ejection, or CME, four planets and the bright stars of the Pleiades cluster are all captured in this image from *SOHO*, taken with the LASCO instrument on 15 May 2000. The CME is seen in the foreground of the 15-degree-wide field of view, leaving the Sun whose position and relative size are indicated by the central white circle. Four of the five naked-eye planets are seen in a rare alignment, as bright disks bisected by a line which is an instrumental effect caused by the intense sunlight reflected from the planet. *SOHO* is about 150 billion meters away from the Sun, while Mercury, Venus, Jupiter and Saturn are, respectively, about 18, 110, 780 and 1400 billion meters beyond the Sun. The Pleiades star cluster is 3.86 million trillion (3.86×10^{18}) meters (408 light-years) away. (Courtesy of the *SOHO* LASCO consortium. *SOHO* is a project of international collaboration between ESA and NASA.)

curvilinear shapes that resemble the cross-sections of loops, shells or filled bubbles, suggesting magnetically closed regions that are sporadically blown out by the eruption. The upper portions of the magnetic loops are sometimes carried out by the highly-ionized material, while remaining attached and rooted to the Sun at both ends. In other situations, the expelled material stretches the magnetic field until it snaps, taking the coiled magnetism with it and lifting off into space like a hot-air balloon that breaks its tether. Whenever a big, closed loop of magnetism is unable to hold itself down, a coronal mass ejection takes off.

Mass ejections erupt from the Sun as self-contained structures of hot material and magnetic fields. They apparently result from a rapid, large-scale restructuring of magnetic fields in the low corona. The spatial distribution of CMEs over the 11-year cycle of magnetic activity is similar to that of the other large structures on the Sun, the coronal streamers and their underlying filaments. Near activity minimum the coronal mass ejections are largely confined to equatorial regions, but near maximum they can be observed at all solar latitudes.

Like sunspots, solar flares and other forms of solar activity, CMEs occur with a frequency that varies in step with the 11-year cycle. A few coronal mass ejections balloon out of the corona per day, on average, during activity maximum, and the rate decreases by about an order of magnitude by sunspot minimum. The rate also depends on the sensitivity of the coronagraph; the *SOHO* LASCO instrument observed

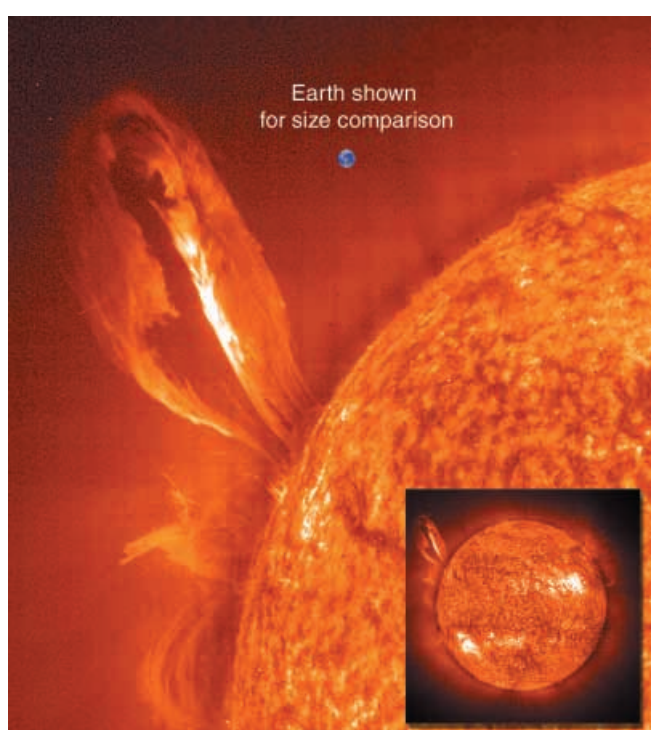

Fig. 6.15 **Eruptive prominence** This large erupting prominence was observed in the extreme-ultraviolet light of ionized helium (He II at 30.4 nm) on 24 July 1999. The comparison image of the Earth shows the enormous extent of the prominence; the inset full-disk solar image indicates that the eruption looped out for a distance almost equal to the Sun's radius. (Courtesy of the *SOHO* EIT consortium. *SOHO* is a project of international collaboration between ESA and NASA.)

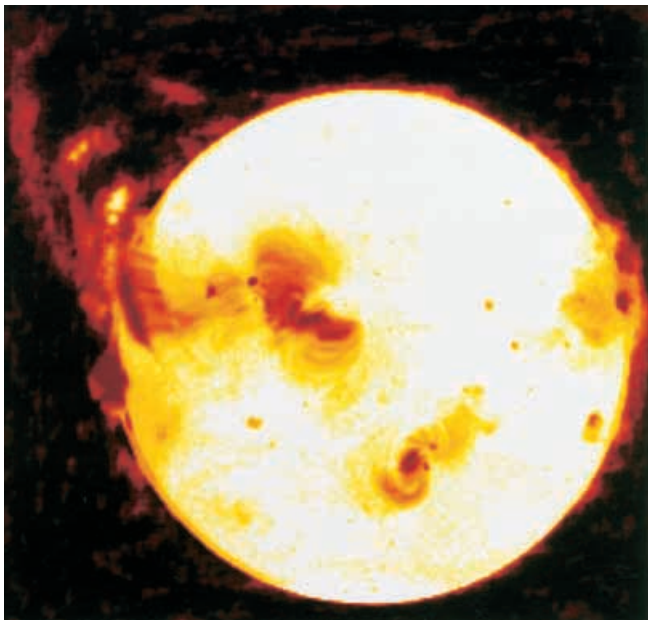

Fig. 6.16 **Stitching up the wound** A time sequence of three radio images show an eruptive prominence above the solar disk at the north-east (*top left*) during a 1.5-hour period. A negative soft X-ray image shows an arcade of loops formed by magnetic reconnection at a slightly later time, as if the Sun was stitching itself back together after the eruption. The radio images are from the Nobeyama Radioheliograph, while the X-ray image was obtained with the Soft X-ray Telescope (SXT) on the *Yohkoh* satellite. (Courtesy of Shinzo Enome, Nobeyama Radio Observatory.)

about 0.8 CMEs per day at activity minimum.

A powerful mass ejection, with its associated shock, energetic particles and magnetic fields, can pummel the Earth's magnetic environment in space, sometimes with devastating consequences for our planet. When it hits the Earth, a mass ejection can produce powerful geomagnetic storms, intense auroras, electrical power blackouts, and other threatening consequences (Section 8.3).

Although CMEs are often observed as magnetic bubbles ejected from one side of the Sun, these events are not likely to collide with the Earth. A coronagraph can detect an Earth-directed CME as a gradually expanding, Sun-centered ring around the Sun. Such a halo coronal mass ejection may signal a future terrestrial hit. Still, you cannot tell from the halo itself whether the mass ejection is targeted for the Earth or moving away from it in the opposite direction.

Coronal mass ejections often exhibit a three-part structure - a smooth, bright outer loop or bubble of enhanced density, followed by a dark cavity of low density, within which sits an erupted prominence. The leading bright loop or shell is the coronal mass ejection that opens up and lifts off like a huge umbrella in the solar wind, piling the corona up and shoving it out like a snowplow. About 70 percent of the coronal mass ejections are associated with, and followed by, eruptive prominences (Fig. 6.15).

The close proximity of coronal mass ejections and erupting prominences in space and time indicates that they are consequences of a similar instability and restructuring of the large-scale (global) magnetic fields in the corona. Restraining coronal magnetic fields may be blown open or carried away by the coronal mass ejection, which precedes the prominence eruption

Quiescent prominences, or filaments, can hang above the photosphere for weeks or months (Section 5.2). Then the supporting magnetism becomes unhinged. The quiescent prominence becomes completely unstable, and it erupts. Instead of falling down under gravity, the stately structures rise up and break away from the Sun, as though propelled by a loaded, twisted spring. The eruptive prominence ascends, and disappears in tens of minutes to several hours. The eruption of an old quiescent prominence is thus sometimes called a *disparition brusque*, French for "sudden disappearance". Some of the prominence material escapes from the Sun, releasing a mass equivalent to that of a small mountain in just a few hours, while some of the material descends to the chromosphere along helical arches.

In two-thirds of the cases, the prominence reforms after the explosive convulsion in the same place and with much the same shape over the course of 1 to 7 days. It is as if some irritation builds up beyond the limit of tolerance, and the magnetic structure tosses off the pent-up frustration, like a dog shaking off in the rain.

Closed magnetic loops apparently support the long, thin prominence, or filament, like parallel hammocks, at heights of up to 100 million meters, or ten times the diameter of the Earth. This arcade of closed loops is anchored in the Sun, but is opened up at the top by the rising filament, like taking the cork out of a bottle of champagne. The magnetism subsequently reconnects and closes up again beneath the erupting prominence, forming a new arcade of closed loops.

We can see the magnetic backbone of an erupting prominence regroup and close up again in soft X-ray images, retaining a memory of its former stability. When the prominence erupts, it is replaced by a row of bright X-ray emitting loops (Fig. 6.16), aligned like the bones in your rib cage or the arched trestle in a rose garden. First observed from *Skylab*, the X-ray loops bridge the magnetic neutral line between opposite polarity regions in the photosphere, stitching together and healing the wound inflicted by emptying that part of the corona.

Yohkoh's Soft X-ray Telescope has investigated these beautiful, arched, post-ejection structures in detail. The loops form progressively from one end of the arcade to the other, and they also rise vertically with time. The enhanced X-ray emission is first seen after the onset of the mass ejection, and remains long after the ejection has departed from the low corona. These long-duration (hours) soft X-ray events, are due to global magnetic restructuring that proceeds along the ejection path.

Roughly 40 percent of coronal mass ejections are accompanied by solar flares that occur at about the same time and place. In fact, the flare-associated, meter-wavelength type II and IV radio bursts suggested the

expulsion of mass from the corona long before coronal mass ejections were discovered using white-light coronagraphs. Yet, the physical size of coronal mass ejections is huge compared with flares or even the active regions in which flares occur. Moreover, the accompanying flares can occur at any time before, during or after the departure or "lift-off" of the mass ejection, and the relative locations of the two phenomena also show no systematic ordering.

So, most mass ejections are not initiated by solar flares and most flares are not caused by the ejections. After all, the flares are much more common. Nevertheless, it seems that the two types of solar explosions do involve similar processes, and they can result from the same magnetic activity in the corona.

What causes the Sun's magnetism to suddenly erupt with enough force to drive a large section of the corona out against the restraining force of solar gravity? The triggering mechanism seems to be related to large-scale interactions of magnetic fields in the low solar corona. This magnetism is always slowly evolving. It is continuously emerging from inside the Sun, and disappearing back into it, driven by the Sun's 11-year cycle of magnetic activity. The release of a coronal mass ejection appears to be one way that the solar atmosphere reconfigures itself in response to these slow magnetic changes. The physical processes involved in storing the magnetic energy in the solar corona and releasing it to launch coronal mass ejections or ignite solar flares are next discussed.

6.3 Theories for explosive solar activity

Powerful solar flares involve the explosive release of incredible amounts of energy, sometimes amounting to as much a million billion billion (10^{24}) joule in just a few minutes. A substantial fraction of this energy goes into accelerating electrons and protons to very high speeds. Comparable amounts of energy are released in expelling matter during a CME, and they are most likely powered by similar processes to those that drive solar flares.

To explain how solar explosions happen, we must first know where their colossal energy comes from. The only plausible sources of energy for these powerful outbursts are the strong magnetic fields in the low solar corona (Focus 6.6). After all, solar flares occur in active regions where the strongest magnetic fields are found. Both solar flares and CMEs are also synchronized with the Sun's 11-year cycle of magnetic activity, becoming more frequent and violent when sunspots and intense magnetic fields are most commonly observed.

Once the source of explosive energy has been established, we must explain where and why that energy is suddenly and rapidly let go. The energy release for solar flares has to occur in the low corona where the energetic particles are accelerated and the magnetic fields are strong enough to provide the necessary energy. Coronal mass ejections similarly require intense magnetic fields to be sufficiently energized, and their enormous size suggests an origin above the photosphere and chromosphere.

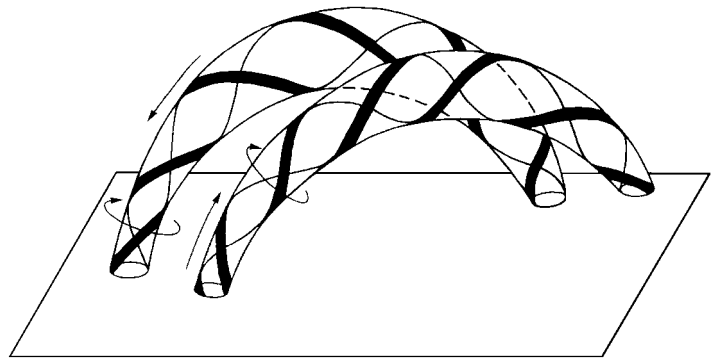

Fig. 6.17 **Magnetic interaction** A pair of oppositely-directed, twisted coronal loops come in contact, releasing magnetic energy to power a solar flare. Arrows indicate the direction of the magnetic field lines and the sense of twist. Such magnetic encounters can occur when newly emerging magnetic fields rise through the photosphere to merge with pre-existing ones in the corona, or when the twisted coronal loops are forced together by underlying motions.

The free magnetic energy needed to power the solar explosions is stored in the low corona in the form of non-potential magnetic field components, or, equivalently, as electric current systems. We can see how this excess "free" magnetic energy might be produced in the corona by considering a magnetic loop that links regions of opposite magnetic polarity or direction in the underlying photosphere. The line dividing the two polarities is called the magnetic neutral line. The magnetic fields have a potential configuration if they connect the two polarities in the shortest, most direct path, and therefore run perpendicular to the magnetic neutral line. They can be distorted into a non-potential shape when motions at or below the photosphere shear and twist the looping fields, creating more magnetic energy than the potential form. This extra energy, called free magnetic energy, can be released during explosions on the Sun.

The free magnetic energy accumulates in the corona, but it comes from the dynamo below. Differential rotation and turbulent convective churning shuffle the photospheric footpoints of coronal loops, and these loops become sheared, twisted and braided. All of this distortion creates large electric current densities and non-potential magnetic fields within the coronal gas.

But what triggers the instability and suddenly ignites the explosions from magnetic loops that remain unperturbed for

Focus 6.6 Energizing solar flares

How much energy is released during a typical solar flare? The total flare energy, E_f, expended in producing electrons with energies, E_e , of about 30 keV, or 4.8×10^{-15} J, within a sphere of R with an electron density of $N_e \approx 10^{17}$ electrons m^{-3} (Focus 6.1) is:

$$E_f = 4\pi R^3 E_e N_e/3 \approx 2 \times 10^{24} \text{ J},$$

where the radius of a compact flare is $R = 10^7$ m, or about twice the Earth's radius. Such a flare subtends an angular radius of 14 seconds of arc when viewed from the Earth.

Magnetic energy stored in the low corona powers these flares. The magnetic energy, E_m , for a magnetic field strength, B, in a radius, R, is:

$$E_m = [4\pi/(6\mu_0)]\, B^2 R^3 = 1.66 \times 10^6\, B^2 R^3 \text{ J},$$

where the permeability of free space is $\mu_0 = 4\pi \times 10^{-7}$ henry m^{-1}, the radius is in meters and the magnetic field strength in tesla. To provide the total flare energy, $E_f = 2 \times 10^{24}$ J in a sphere of radius $R = 10^7$ m, a magnetic field of about 0.03 tesla is required. Solar astronomers often use the c.g.s. unit of gauss, where 1 gauss = 10 000 tesla, so the required magnetic field change in the corona is roughly 300 gauss. Lower magnetic field strengths might suffice if the volume is larger and the electron density smaller.

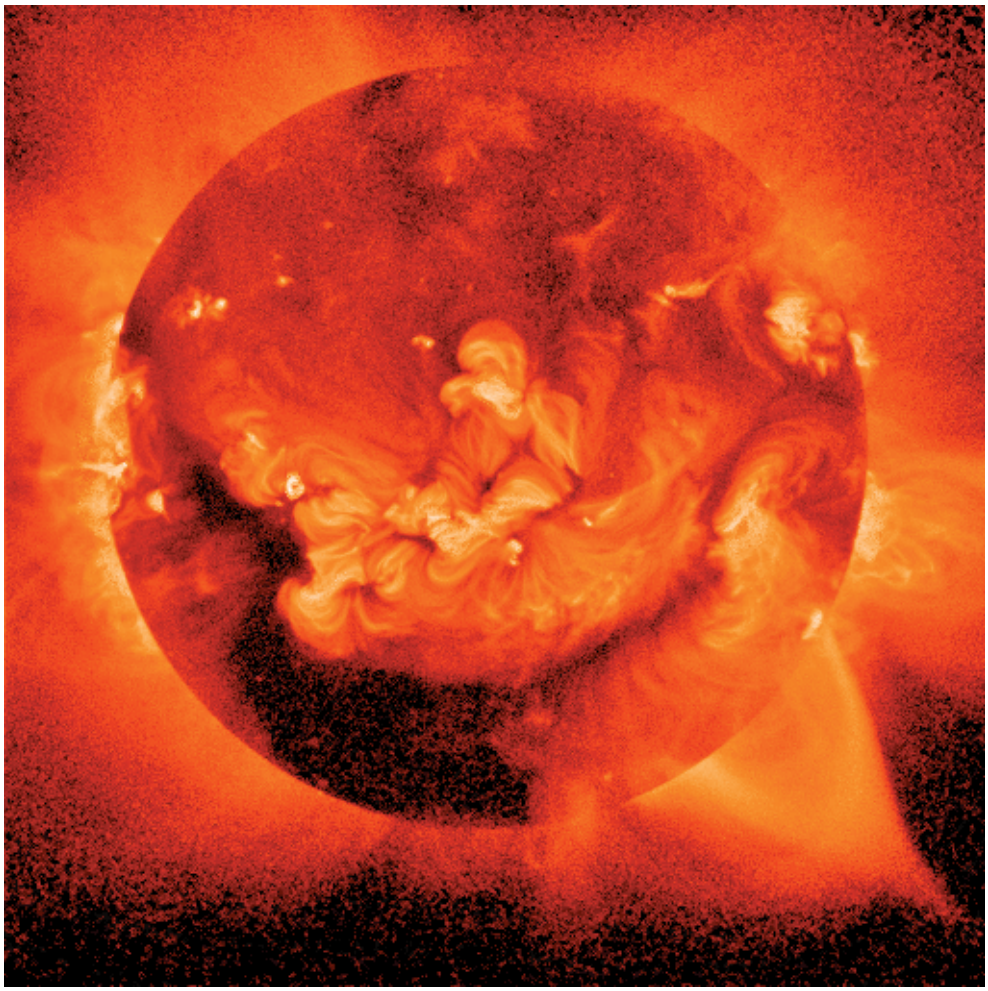

Fig. 6.18 **Cusp geometry** A large, soft X-ray cusp structure (*lower right*) is detected after a coronal mass ejection on 25 January 1992. The cusp, seen edge-on at the top of the arch, is the place where the oppositely-directed magnetic fields, threading the two legs of the arch, are stretched out and brought together. Several similar images have been taken with the Soft X-ray Telescope (SXT) aboard *Yohkoh*, showing that magnetic reconnection is a common method of energizing solar explosions. (Courtesy of Loren W. Acton, NASA, ISAS, the Lockheed-Martin Solar and Astrophysics Laboratory, the National Astronomical Observatory of Japan, and the University of Tokyo.)

long intervals of time? They might be triggered when magnetized coronal loops, driven by motions beneath them, meet to touch each other and connect (Fig. 6.17). If magnetic fields of opposite polarity are pressed together, an instability takes place and the fields partially annihilate each other. Nevertheless there is still some magnetism left. The magnetic field lines are never permanently broken, and they simply reconnect into new magnetic configurations. The non-potential components of the magnetic fields are destroyed in this reconnection process, and their free magnetic energy is used to energize solar explosions.

So, we now think of these powerful outbursts as stemming from the interaction of coronal loops. They are always moving about, like swaying seaweed or wind-blown grass, and existing coronal loops may often be brought into contact by these movements. Magnetic fields coiled up in the solar interior, where the Sun's magnetism is produced, could also bob into the corona to interact with pre-existing coronal loops. In either case, the coalescence leads to the rapid release of free magnetic energy through magnetic reconnection.

The explosive instability has been compared to an earthquake. According to this analogy, the moving roots or footpoints of a sheared magnetic loop resemble two tectonic plates. As the plates move in opposite directions along a fault line, they grind against each other and build up stress and energy. When the stress is pushed to the limit, the two plates cannot slide further, and the accumulated energy is released as an earthquake. That part of the fault line then lurches back to its original, equilibrium position, waiting for the next earthquake. After an explosive convulsion on the Sun, the magnetic fields similarly regain their composure, fusing together and becoming primed for the next outburst.

The rapid, explosive loss of equilibrium has additionally been compared to avalanches in a sand pile or on a ski slope, to the quick snap of a rubber band that has been twisted too tightly, and to the sudden flash and crack of a lightening bolt.

The Soft X-ray Telescope, or SXT, aboard the *Yohkoh* spacecraft has demonstrated that magnetic interactions can indeed strike the match that ignites solar explosions. Sequential SXT images indicate that magnetized loops can become sheared and twisted, while also converging within active regions or on larger scales. SXT also witnessed the coalescence of emerging, twisted loops with overlying ones. The magnetic distortions suggest the build up of energy that is dissipated at the place where the loops meet.

Yohkoh's SXT even revealed the probable location of the magnetic reconnection site, showing that the rounded magnetism of a coronal loop can be pulled into a peaked shape at the top (Fig. 6.18). The sharp, cusp-like feature marks the place where oppositely directed field lines stretch